Yale 耶鲁大学-南京信息工程大学大气环境中心

Yale-NUIST Center on Atmospheric Environment

A discussion on the paper "Evaporation from Lake Superior: 1.Physical controls and processes"

By Peter D.Blanken

Liu Qiang

2016.10.14

Outline

- Introduction
- Methodology
- Results and discussion
- Conclusions

Introduction

- 1. The socioeconomic importance of the Great Lakes: directly; indirectly.
- 2. Past research on the surface energy balance of the Great Lakes: empirical models; buoy-based measurements; hydrodynamic models.
- 3. The Lake Superior's responding to climate change: temperature; wind ;water levels; ice cover.

Methodology

$$J_s = R_n - \lambda E - H$$

$$\lambda E = \overline{\lambda w' q'}$$

$$H = \overline{\rho c w' T'}$$

$$R_n = S\downarrow(1-\alpha) + L\downarrow - L\uparrow$$

(α sets to 0.07 when ice-free;0.8 when ice-covered)

$$L\uparrow = \varepsilon\sigma T_0^4$$

(ε is the Stefan-Boltzmann constant; σ is 0.98)

$$\zeta = z/L$$

(z is the measurement height of 32.4m,L is the Oabukhov stability length)

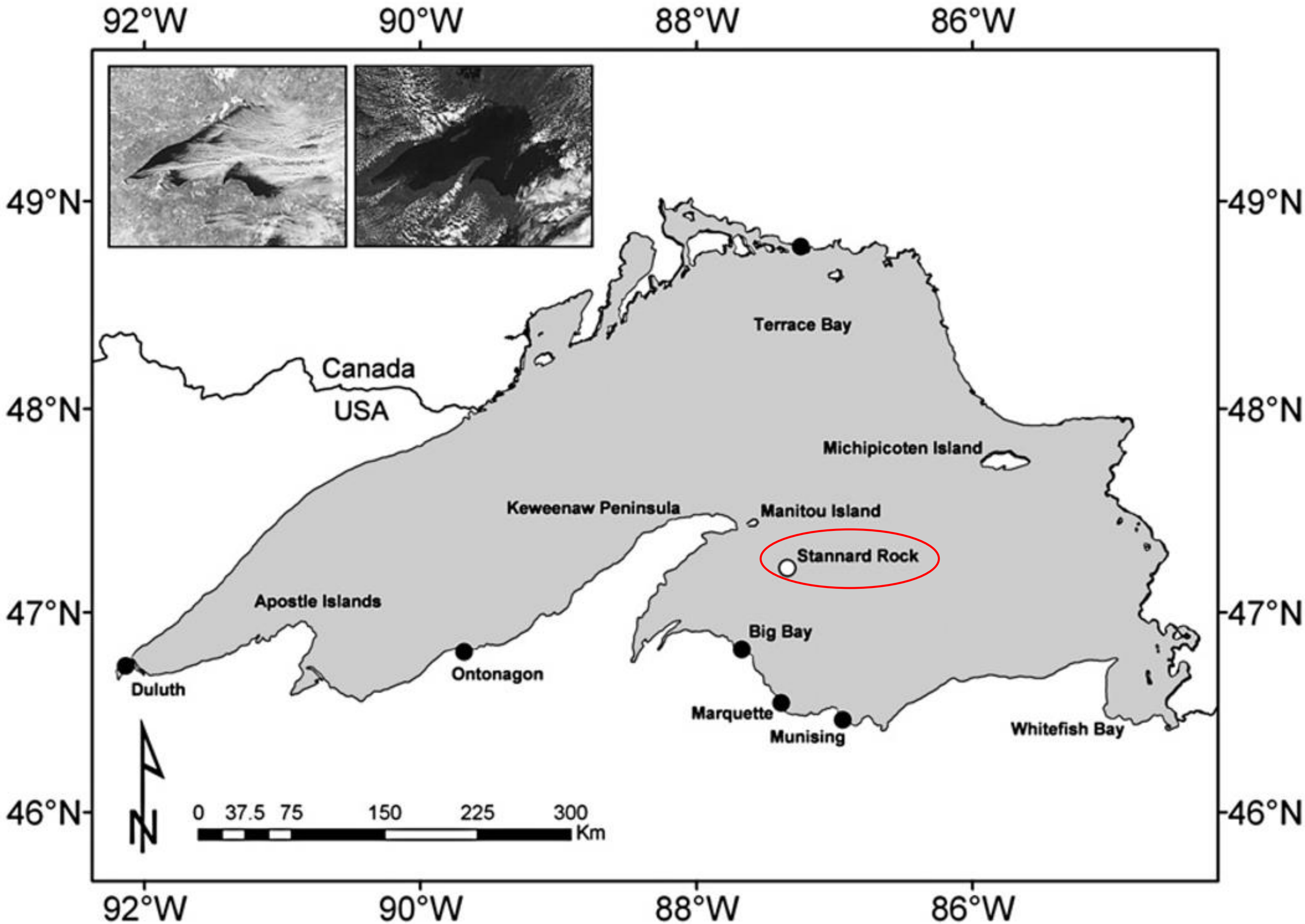

Fig. 1. Map of Lake Superior. The location of Stannard Rock is identified.

Result and discussion

1.Seasonal pattern

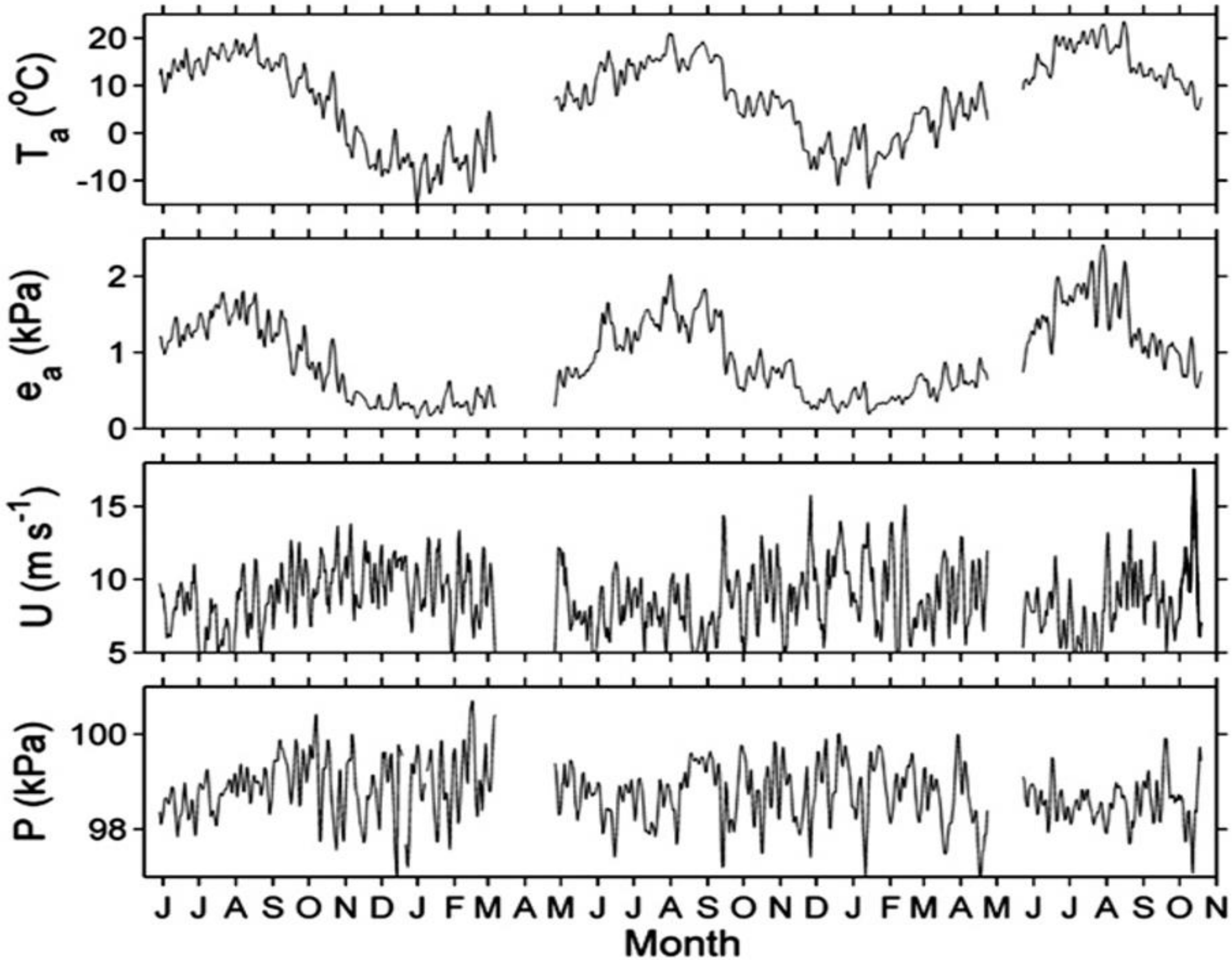

（Std dev
0.51kPa in JJA；
0.92kPa in DJF）

Fig. 2. Three-day running means of half-hour measurements of basic meteorological conditions from June 12, 2008 through November 4, 2010; air temperature (T_a), vapor pressure (e_a), horizontal wind speed (U), barometric pressure (P). Mid-months are labeled.

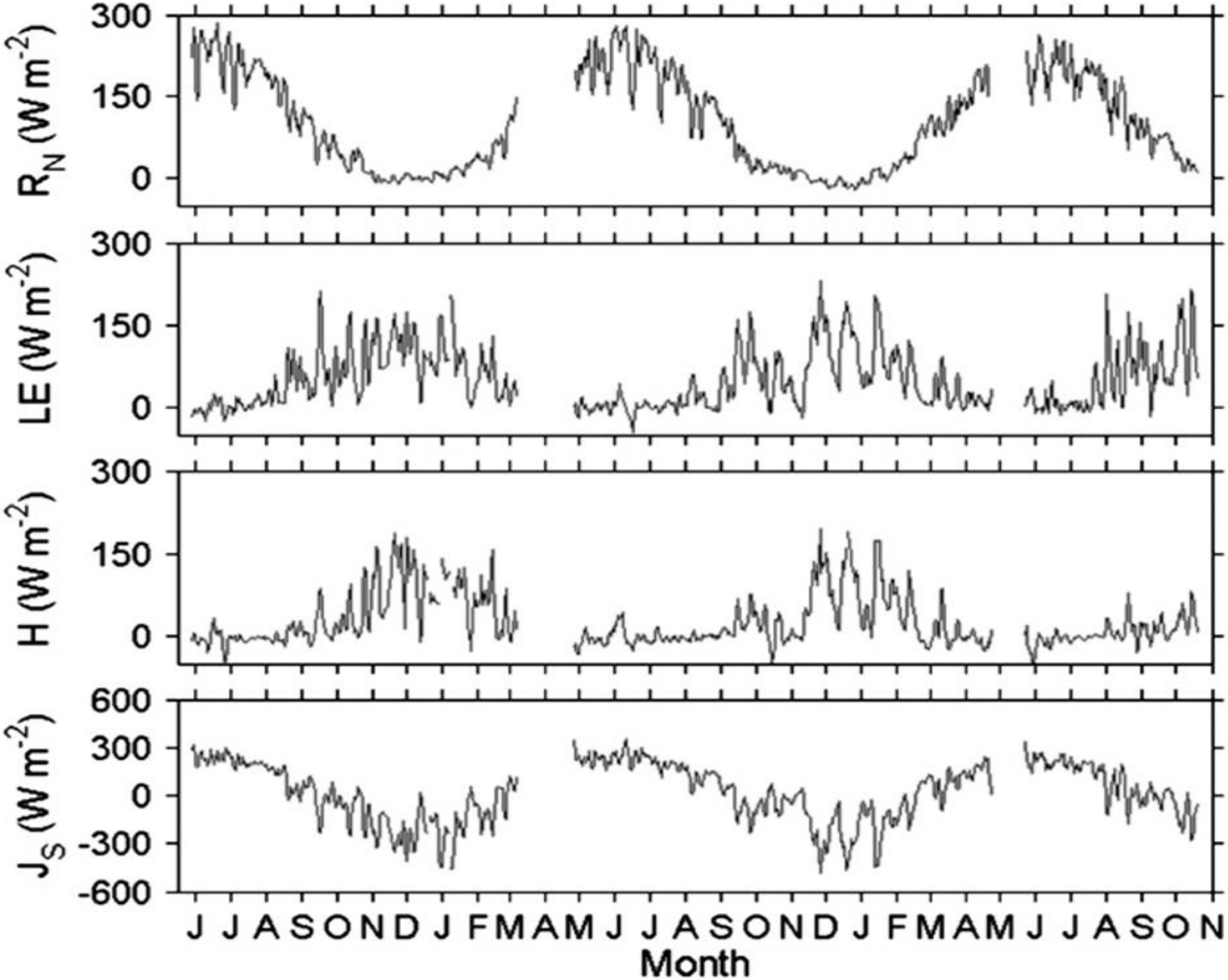

Fig. 3. Three-day running means of half-hour measurements of the surface energy balance from June 12, 2008 through November 4, 2010; net radiation (R_N), latent heat flux (λE), sensible heat flux (H), energy storage estimated as the residual of the energy balance (J_S). Mid-months are labeled.

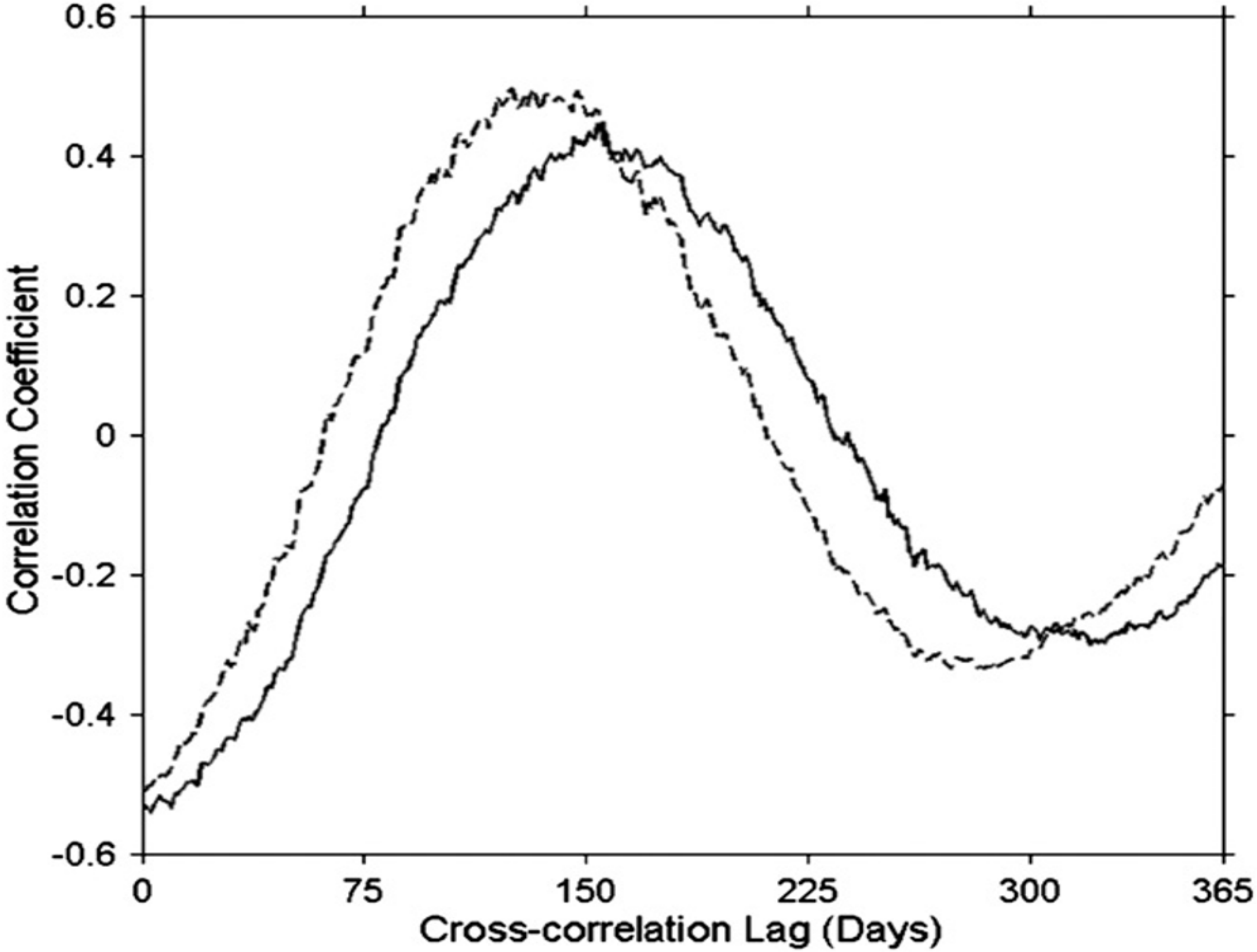

Fig. 4. Cross-correlations between the 24-h mean linear detrended net radiation and latent heat flux (λE; solid line); and the 24-h mean linear detrended net radiation and sensible heat flux (H; dashed line). Maximum correlation coefficients were obtained with a lag of 147 and 154 days for H and λE, respectively.

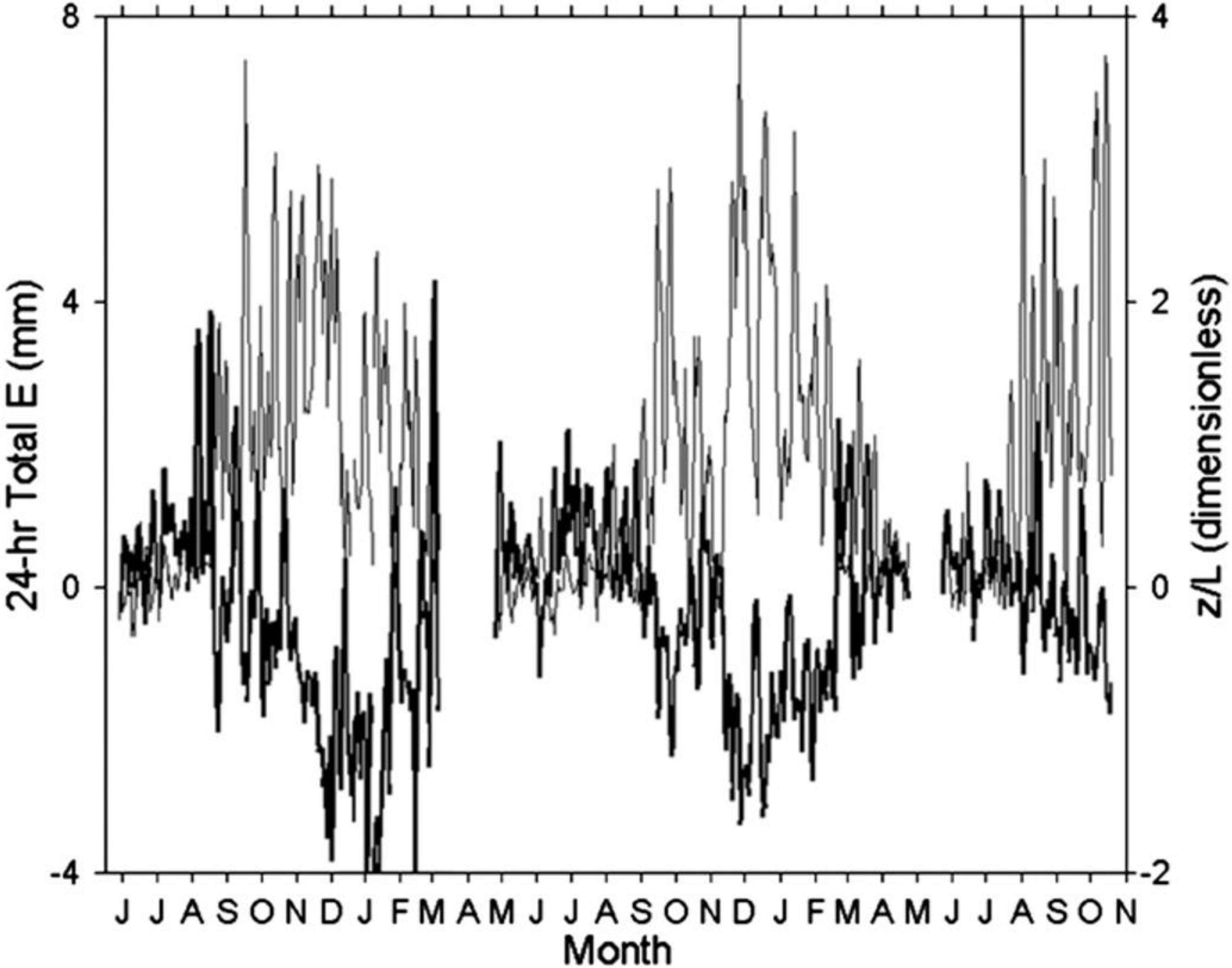

Fig. 5. Three-day running means of the 24-h total evaporation (thin lines) and the Obukhov stability parameter ζ=z/L (thick lines; positive=stable; negative=unstable) from June 12, 2008 through November4, 2010. Mid-months are labeled.

2.Phiscal process

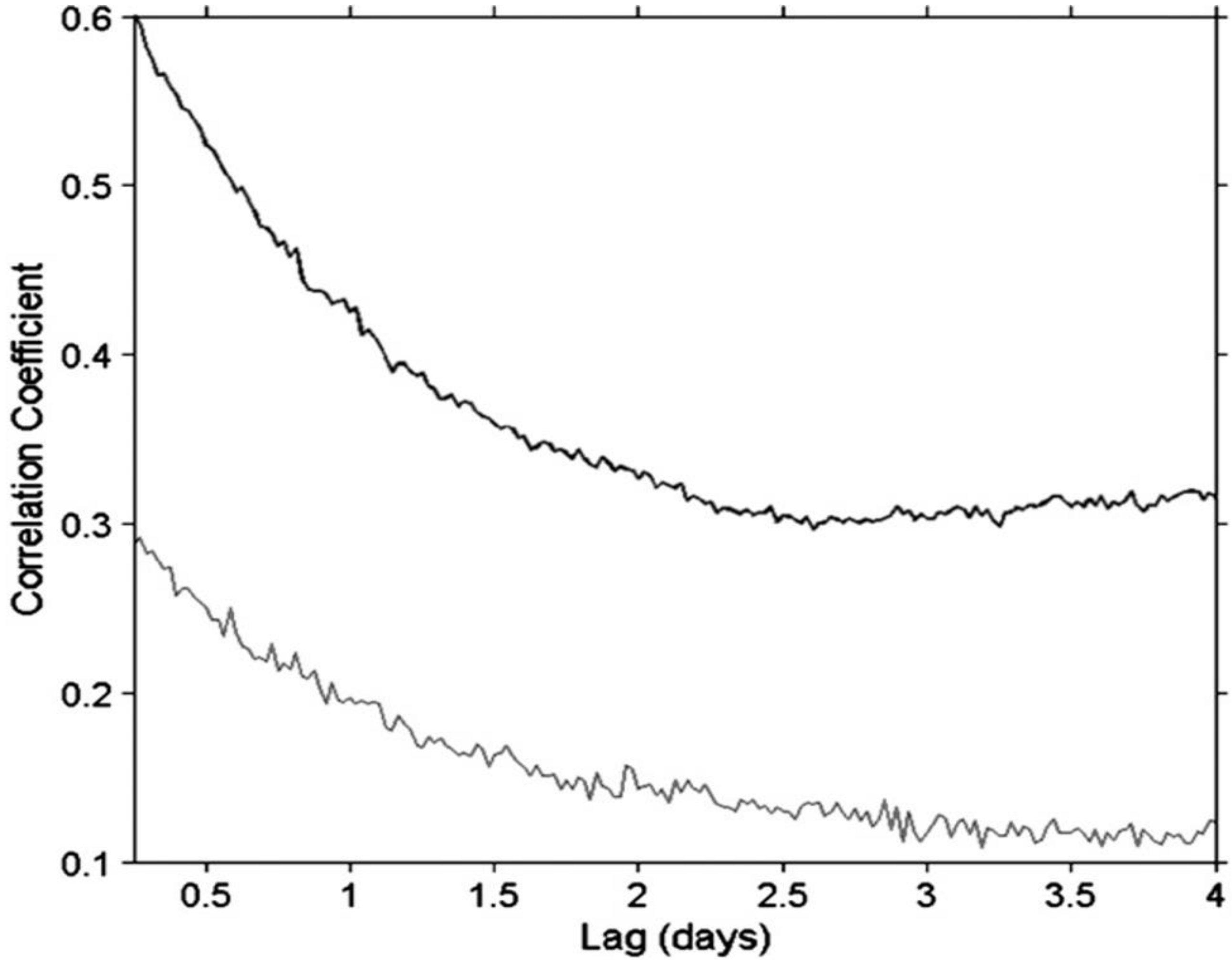

Fig. 6. Correlation coefficient(r) for the linear detrended lagged autocorrelation sequence for the sensible heat flux (thick line) and the latent heat flux (thin line) for all of the 0.5-h measurements taken over from June 12,2008 through November 4, 2010. For clarity, plot starts at a lag of 0.25 days following the sharp decrease from r=1 at lag=0 days.

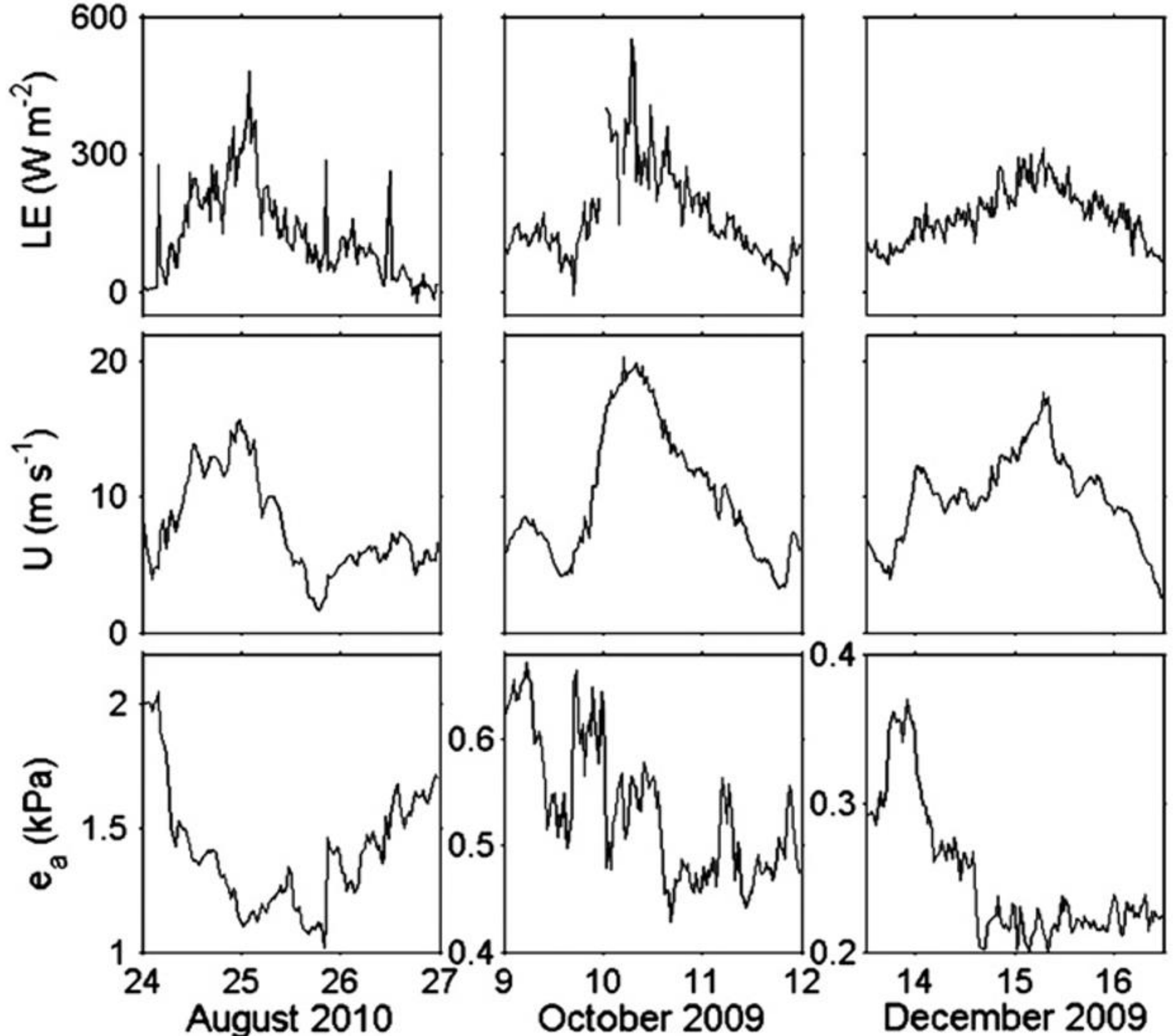

Fig. 7. Three examples of typical three-day evaporation events along a gradient of vapor pressures from high (12:00pm August 24–12:00 pm August 27, 2010 EDT), to medium (12:00pm October 9–12:00pm October 12, 2009 EDT), to low (12:00am December 14–12:00am December 17, 2009 EDT). Half-hour means of the latent heat flux (λE), horizontal wind speed (U), and vapor pressure (e_a) measured at 32.4-m above the mean water surface, are shown.

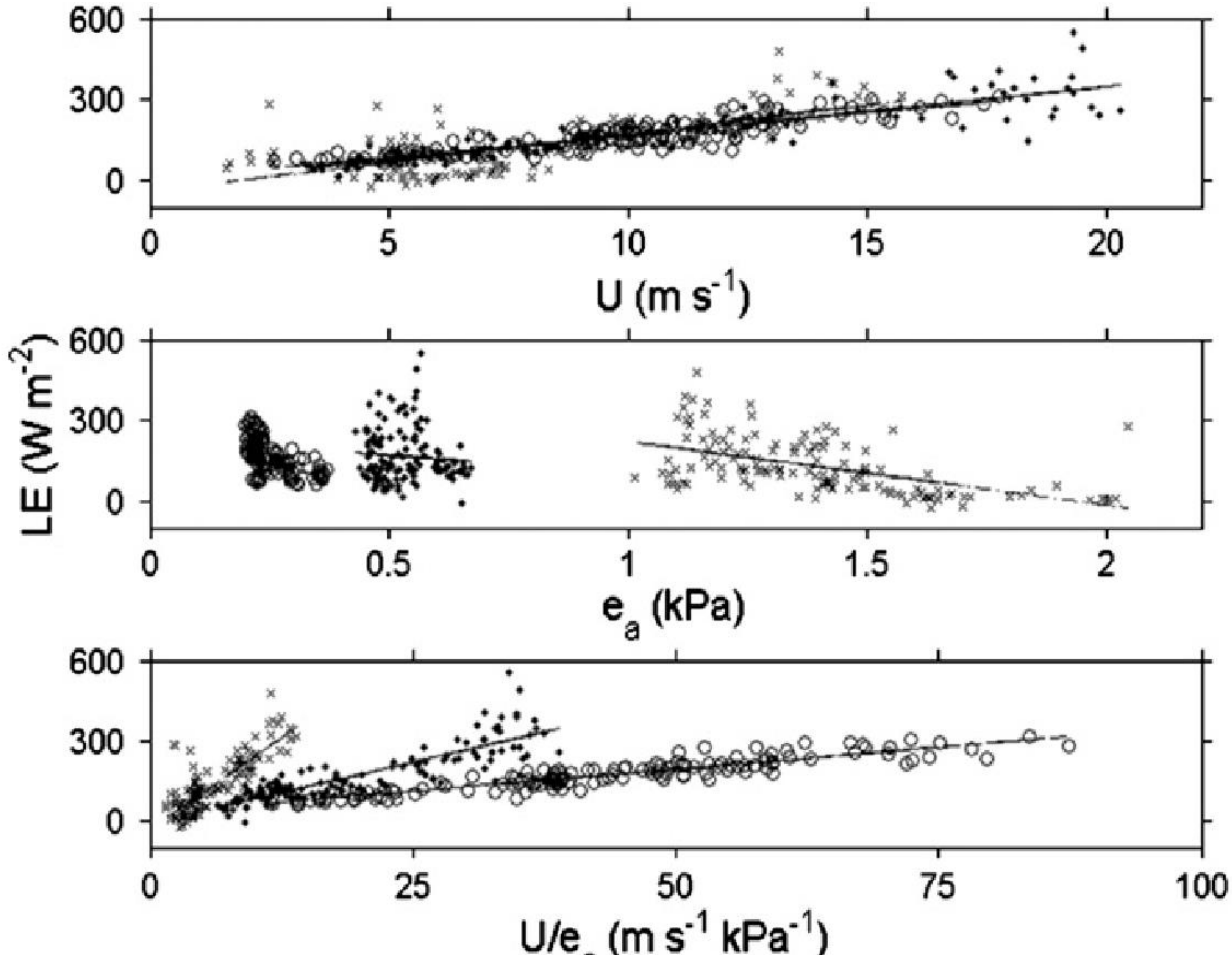

Fig. 8. Scatter plot (points) with linear regressions (lines) showing the relationship between the 0.5-h latent heat flux (λE) and the 32.4-m horizontal wind speed (U), vapor pressure (e_a) and ratio U/e_a. Shown are three example evaporation events (see Fig.8) that occurred during October9–12,2009 (solid circles; solid lines), December 14–17, 2009(open circles; dashed lines),andAugust24–27,2010 (crosses; dotted lines)

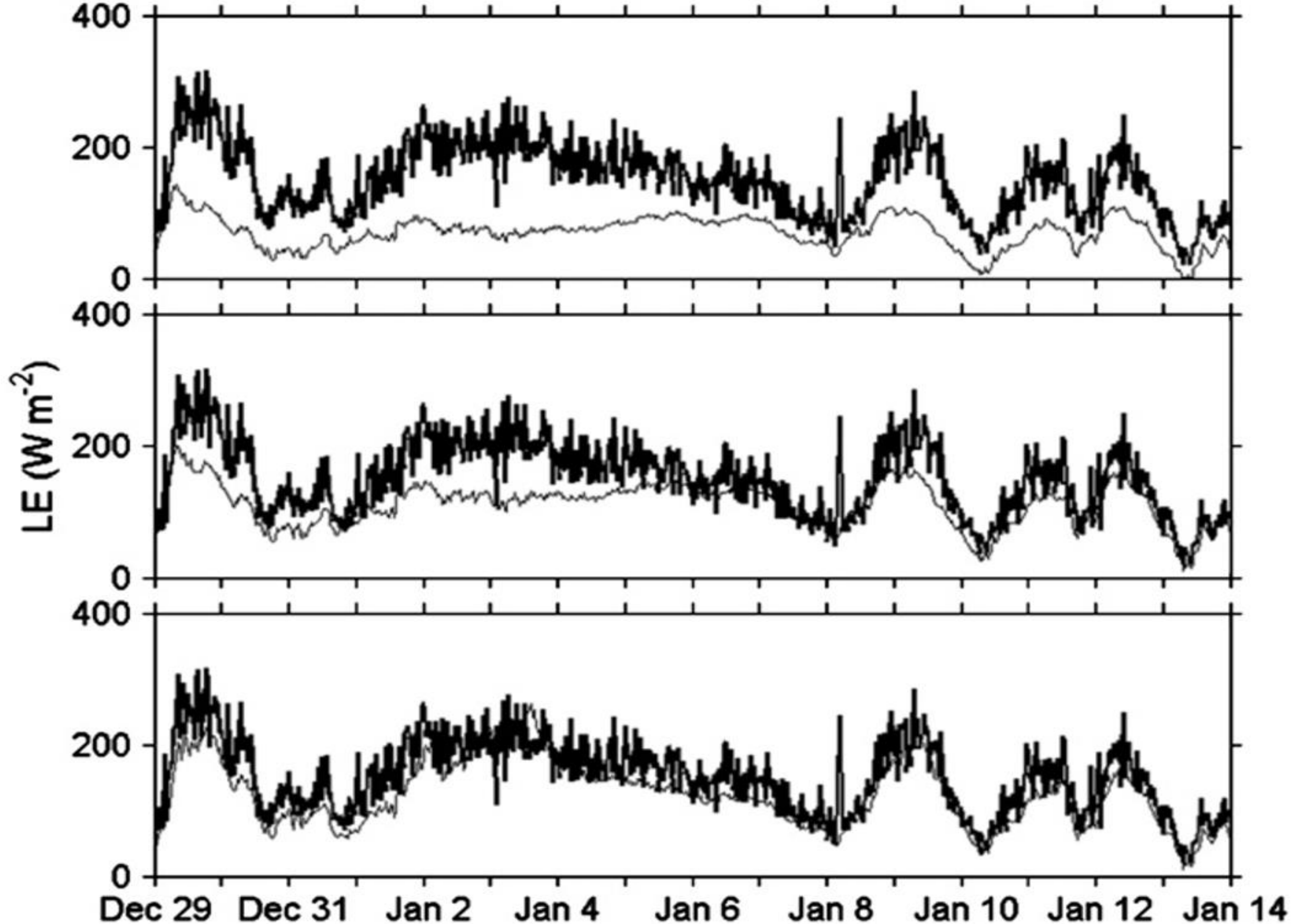

Fig. 9. Measured (thick lines) and modeled (thin lines) 30-min mean latent heat fluxes from December 29, 2009 through January 14, 2010. Modeled λE were based on linear regressions of λE against horizontal wind speed (U; top panel), λE/U against vapor pressure (e_a; middle panel), and λE against U/ea (bottom panel) using all of the measured data. See Table 3 for summary statistics.

3.The relationship between ice cover and evaporation

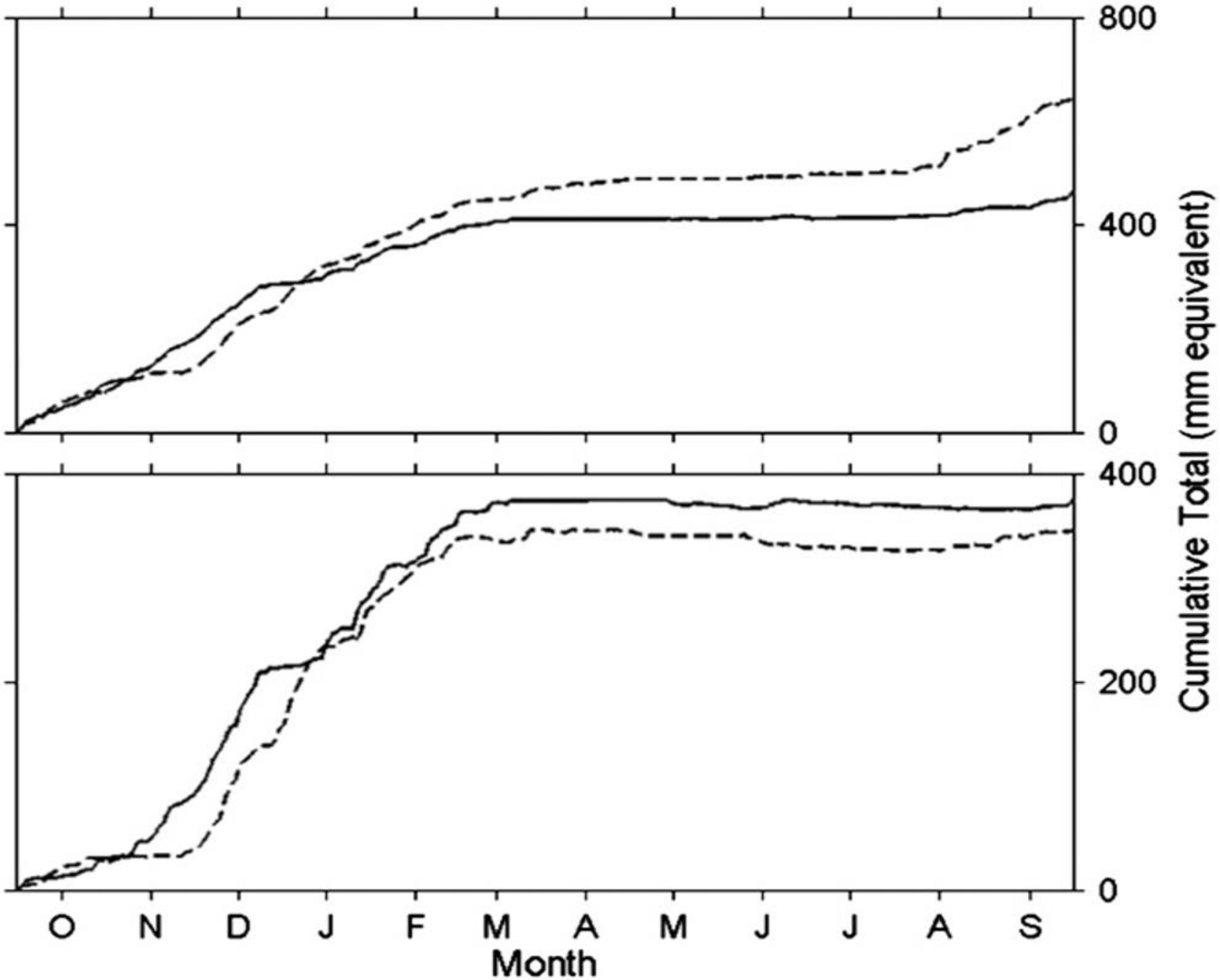

Fig. 10. Cumulative 0.5-h latent heat flux (top) and sensible heat flux (bottom) expressed as equivalent mm of water for the period October 1st through September 30th of 2008–2009 (solid line) and 2009–2010 (dashed line). Mid-months are labeled.

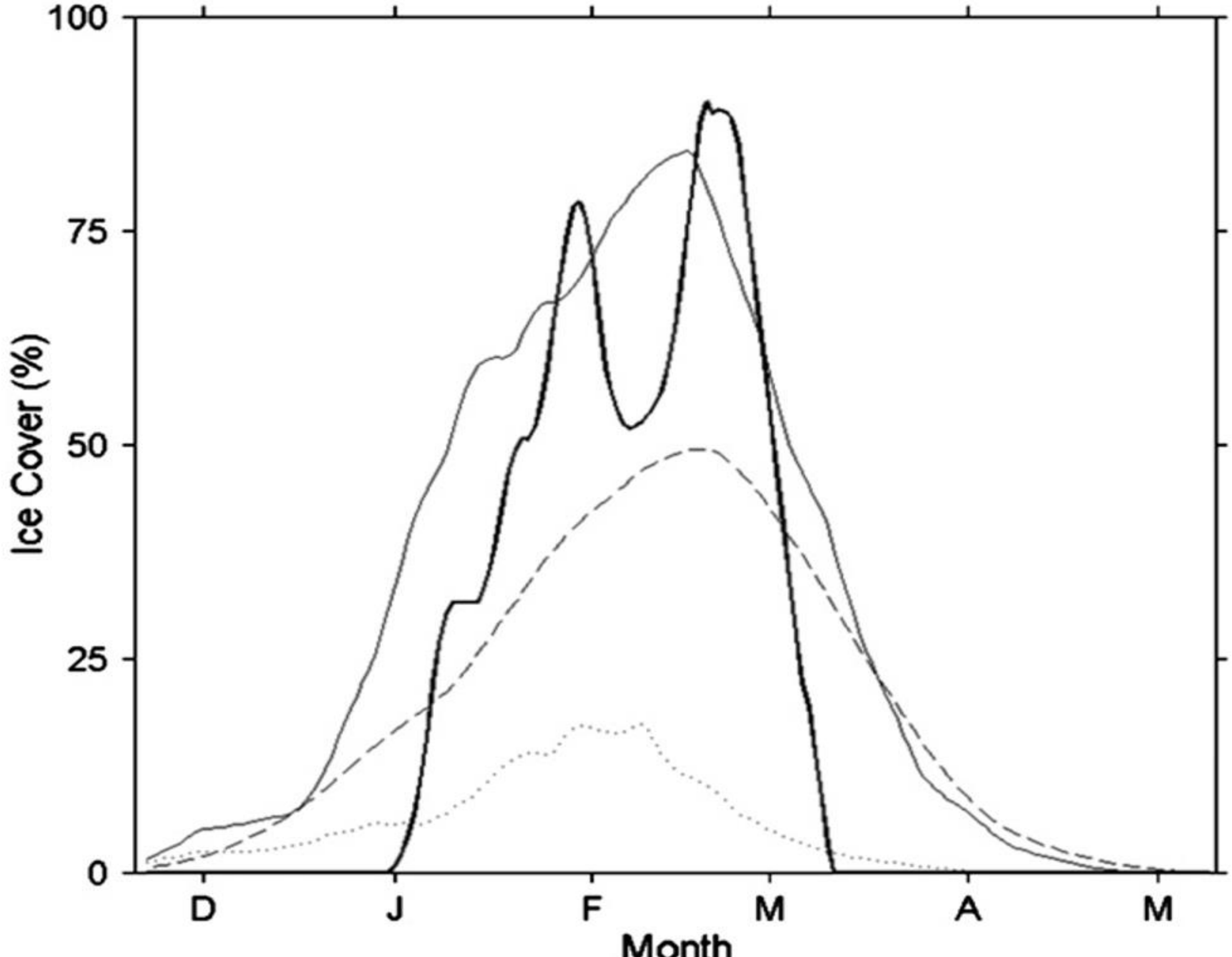

Fig. 11. 15-day running means of the percentage of the lake-wide ice cover for 2008–2009 (thin solid line), 2009–2010 (dotted line), and the 1973–2010 climatological mean (dashed line). Ice cover within the turbulent flux footprint radius (6km) for 2008–2009 (thick solid line). No ice was present within the 6-km radius during 2009–2010. Mid-months are labeled.

2008-2009

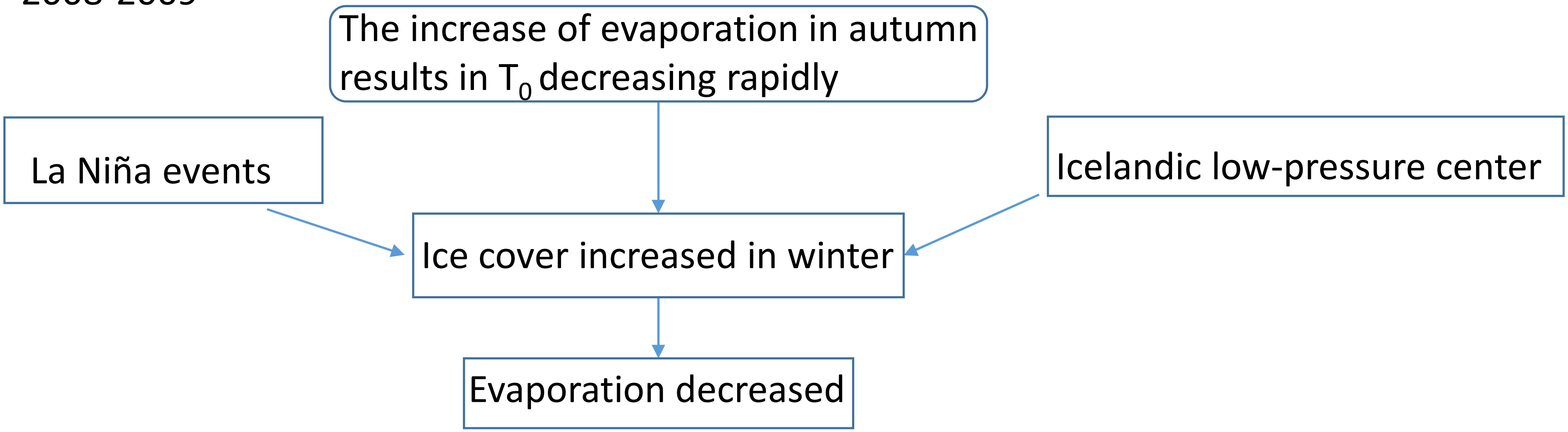

2009-2010

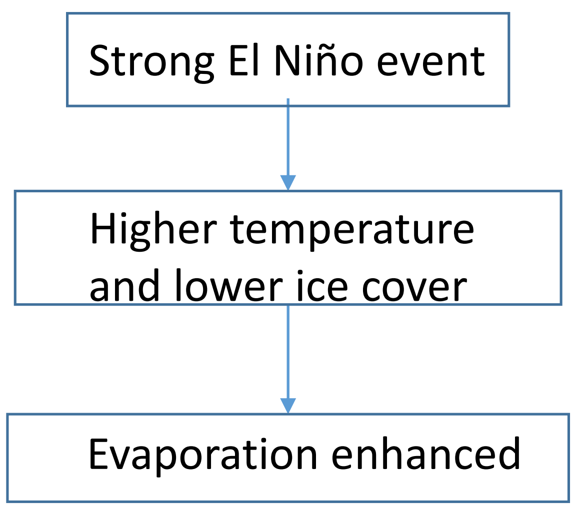

4.The possible response to climate change

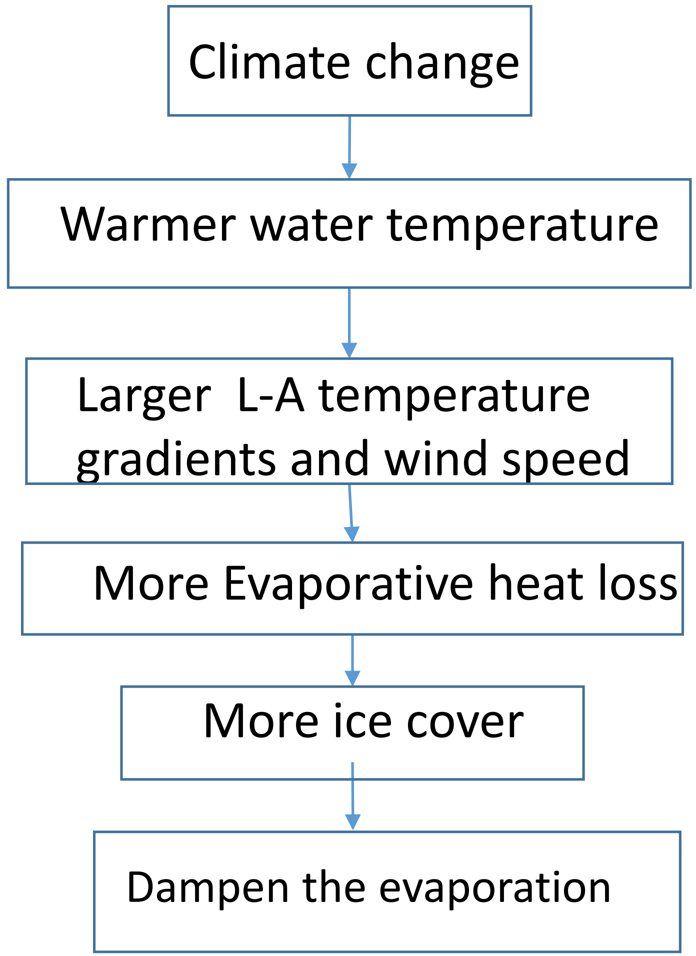

Conclusion

- The majority of the evaporative and sensible heat loss occurred during the autumn and winter, with evaporation proportional to the horizontal wind speed, inversely proportional to the ambient vapor pressure.
- The five-month delay between maximum summertime energy inputs and wintertime energy outputs indicates that the energy source for the winter season heat loss is the internal energy of the lake itself.
- Evaporative and sensible heat losses act as negative feedbacks to dampen further warming and reductions in ice cover, particularly in near-shore regions.

- We anticipate changes in evaporation and ice cover on two time scales. In the short term (e.g., decades), warming will likely result in increased summer evaporation due to higher surface water temperatures and higher wind speeds, while winter evaporation will likely increase in response to decreased mid-lake ice coverage.
- Over the long term (e.g., centuries) evaporation in the summertime may increase to such an extent that the evaporative seasonal cycle becomes significantly dampened, even in the complete absence of winter ice cover.

THANK YOU